

Date of publication xxxx 00, 0000, date of current version xxxx 00, 0000.

Digital Object Identifier 10.1109/ACCESS.2017.DOI

Imitation Learning for Variable Speed Object Manipulation

Sho SAKAINO¹, (Member, IEEE), Kazuki FUJIMOTO², (Non Member), Yuki SAIGUSA³, (Non Member), and Toshiaki TSUJI², (Senior Member, IEEE)

¹Faculty of Engineering, Information and Systems, Department of Intelligent Interaction Technologies, University of Tsukuba, Japan

²Electrical and Electronic Systems, Saitama University, Saitama, Japan

³Graduate School of Science and Technology, Degree Programs in Intelligent and Mechanical Interaction Systems, University of Tsukuba, Japan.

Corresponding author: Sho Sakaino (e-mail: sakanio@iit.tsukuba.ac.jp).

This work was partly supported by the Adaptable and Seamless Technology Transfer Program through Target-driven R&D (A-STEP) from the Japan Science and Technology Agency (JST) Grant Number JPMJTR20RG.

arXiv:2102.10283v2 [cs.RO] 17 May 2021

ABSTRACT To operate in a real-world environment, robots have several requirements including environmental adaptability. Moreover, the desired success rate for the completion of tasks must be achieved. In this regard, end-to-end learning for autonomous operation is currently being investigated. However, the issue of operating speed has not been investigated in detail. Therefore, in this paper, we propose a method for generating variable operating speeds while adapting to perturbations in the environment. When the work speed changes, there is a nonlinear relationship between the operating speed and force (e.g., inertial and frictional forces). However, the proposed method can be adapted to nonlinearities by utilizing small amount of motion data. We experimentally evaluated the proposed method for erasing a line using an eraser fixed to the tip of a robot. Furthermore, the proposed method enables a robot to perform a task faster than a human operator.

INDEX TERMS Imitation learning, bilateral control, motion planning, fast-forward, machine learning

I. INTRODUCTION

The utilization of machines and robots is pervasive in some industrial fields. In the future, it is expected that robots will replace most of the processes in factory automation or housework. However, at present, many processes are still performed manually, and labor is not yet fully automated because robots lack adequate environmental adaptability. There are two main ways to improve adaptability: hardware and software improvements. An example of the former solution involves gripping objects. Suction hands are often used in the Amazon Picking Challenge, in which the manipulation of multiple objects with different sizes, shapes, and stiffnesses is required [1]. Another example of the former solution is the use of jamming hands [2]. These hands have flexible bags and structures filled with powder. In addition, they grip objects by vacuuming the powder in the bags. Although these hands have certain adaptability to different objects, their ability to grip an object is limited by the physical characteristics of the hardware.

The second solution, the software approach, has also been extensively studied. Levine *et al.* succeeded in gripping various objects using reinforcement learning (RL) based on end-to-end learning [3]. However, this approach is impractical

because the model learns via 800,000 repetitive trials using actual machines. Given that robotic control involves interactions with a real-world environment, the time required for a single trial is constrained by the time constant of the physical phenomenon under investigation. Hence, applying RL from the onset requires an impractical trial time. Imitation learning, which can address this problem, is gaining attention. In this process, humans provide demonstrations as teacher data, and the robots mimic the human motion. This approach significantly reduces the number of trials required. Many studies have demonstrated the effectiveness of imitation learning by applying Gaussian mixture models [4] [5], neural networks (NNs) [6] [7], and RL [8]. Some researchers have reported visual imitation learning [9]. Imitation learning using force information has also attracted notable attention owing to its high adaptability to environmental changes [10]–[14].

However, such imitation learning is focused on performing geometrically challenging robotic tasks and is not relevant to reproducibility over time, such as in the case of a phase delay. As a result, the movements are often static and slower than human operations, and it is difficult to realize movements based on the dynamic interaction between robots and objects.

Motion that considers friction and inertial forces, such as that described in [15], remains a challenging problem. Conventional imitation learning predicts the next response value of a robot and provides it as a command value. In general, no ideal control system exists, and a delay between the command value and the response value occurs. As a result, only low-speed operation, wherein control systems can be assumed to be ideal, can be achieved. As such, robots cannot move faster than humans in tasks that involve the manipulation of unknown objects.

We recently showed that this problem can be solved using four-channel bilateral control [16] [17]. Bilateral control is a remote operation that synchronizes two robots: a master and a slave. Furthermore, four-channel bilateral control is a structure with a position controller and a force controller implemented on both robots [18] [19]. Using bilateral control, an operator can experience control delay on the slave side and dynamic interaction with the environment. Thus, the operator can compensate for the control delay and dynamic interaction. There is no novelty in imitation learning using bilateral control [20] [12]. However, even if bilateral control is used, it is inadequate. We revealed that the teacher data obtained via bilateral control can be fully utilized under the following three important conditions:

1) Predicting the master robot's response

When the response of a certain slave is measured, the command in the next step must be predicted. In the case of bilateral control, the response value of a master is given as the command value of a slave, and the command value can be directly measured. Note that this command value includes human skills to compensate for control delays and dynamic interactions.

2) Having both position and force control in a slave

Position control is robust against force perturbations, and force control is robust against position perturbations. Although robot control can be described as a combination of these controls [21], the predominant control is task-dependent and often not obvious. In this case, machine learning must apply a configuration that can adjust to both position and force commands.

3) Maintaining control gains

Research has also been conducted on adjusting control gains to achieve environmental adaptability [22]. However, if the control gains are changed, the dynamic characteristics of the control also change. Robots are then unable to mimic the skills of humans and compensate for control delays and dynamic interactions. In summary, the controllers must be consistently applied when the training data are collected and during autonomous execution.

Our method satisfies these requirements, and the control system does not need to be ideal because the operation is performed by explicitly considering the control delay by predicting the response of the master. Therefore, it is possible to realize object operation at a rate comparable to that of

humans, and high adaptability to environmental changes is achieved. A detailed explanation can be found in the references [23] [24].

Given that fast motion can be achieved using the proposed method, a generalization ability with respect to operating speed is the next target. A basic study on achieving variable operating speed was proposed by Yokokura *et al.* [25], in which a robot moved autonomously by reproducing stored motion. A reproduced motion was generated using a simple linear interpolation and extrapolation of the stored motion. However, this method has been evaluated only in highly transparent single-degree-of-freedom (DOF) linear motors. In actual multi-DOF robots, dynamic forces, such as an inertial force, change significantly according to the operating speed. The required state of the end-effector also differs depending on the operating speed because the pressing force on the paper surface is adjusted to utilize inertial force during high-speed operation, and the eraser is actively pressed against the paper surface during low-speed operation. The force and operating speed clearly have a nonlinear relationship. However, it should be possible to express this relationship using specific functions.

In this paper, we propose a method in which the operating speed is varied using imitation learning based on four-channel bilateral control. Note that, in the proposed method, the operating speed can even exceed that of the original demonstrations. If a robot can be moved quickly, the productivity of a factory can be improved. Moreover, it is also desirable to adjust the operating speed to match the production speed of other production lines. To evaluate the effectiveness of the proposed method, we performed a task in which a robot erased a line written in pencil using an eraser fixed to the robot. Utilization of the relationship between the inertial force, friction force, and operating speed is necessary to accomplish this task because a large operating force is required for fast operation to compensate for the inertial force, and vice versa. Moreover, even when the same task is performed, a different operating force is required depending on the operating speed because the friction characteristics change significantly with speed. Using the proposed method, the operating speed is determined based on the peak frequency calculated using the fast Fourier transform (FFT), and the slave responses are concatenated and inputted into an NN. Variable speed operation is achieved by simply incorporating the operating frequency as an input, even though the method is almost identical to that described in [16] [17]. The proposed method can be regarded as a combination of imitation learning with parametric biases, in which the physical parameters of robotic motions can be adjusted [26]. This illustrates the high generalization capability of our approach. The validity of the proposed method was experimentally evaluated.

Note that it is not difficult to achieve a variable speed of movement for manipulation of previously known objects or faster movement compared to humans. In addition, it is not difficult to slowly manipulate unknown objects. Therefore,

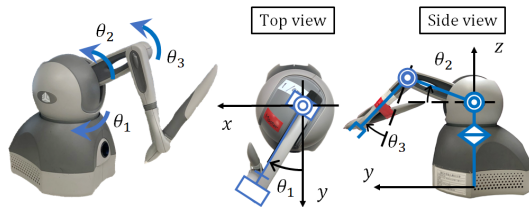


FIGURE 1. Definition of the robot's joints and Cartesian coordinates

TABLE 1. Identified system parameters

J_1	Joint 1 inertia [m Nm]	3.49
J_2	Joint 2 inertia [m Nm]	3.36
J_3	Joint 3 inertia [m Nm]	1.06
D	friction compensation coefficient [$\text{mk} \text{g m}^2/\text{s}$]	12.1
G_1	Gravity compensation coefficient 1 [m Nm]	124
G_2	Gravity compensation coefficient 2 [m Nm]	51.6
G_3	Gravity compensation coefficient 3 [m Nm]	81.6

the contributions of this investigation are summarized as follows:

- Variable speed object manipulation of unknown objects
- Manipulation of unknown objects at a speed equal to or faster than that of human demonstrations

The remainder of this paper is organized as follows. Section 2 describes the robot control system and the bilateral control used in this study. Section 3 describes the proposed learning method and the detailed network structure. Section 4 details the experiment and the results, in addition to a description of a comparative experiment involving the proposed method and a variable-speed motion copy approach based on the study described in [25]. Finally, Section 5 presents the concluding remarks and areas of future study.

II. ROBOT AND CONTROLLER

In this section, the robots and controllers used in this study are described.

A. SETUP

In this study, we used two Geomagic Touch haptic devices manufactured by 3D systems (Rockhill, SC, USA) as manipulators (Fig. 1). Two robots were used during the data collection phase, and an autonomous operation phase using an NN model was executed using a single robot. The robot's joints and Cartesian coordinates are defined as shown in Fig. 1. The model of the robots was assumed to be the same as that in [24]. However, the physical parameters of the robot were different and were identified on the basis of [27]. Table 1 shows the physical parameter values used in this study. The parameters J , D , and G are the inertia, friction compensation coefficient, and gravity compensation coefficient, respectively. The parameters with subscripts 1, 2, and 3 represent those of the first, second, and third joints, respectively.

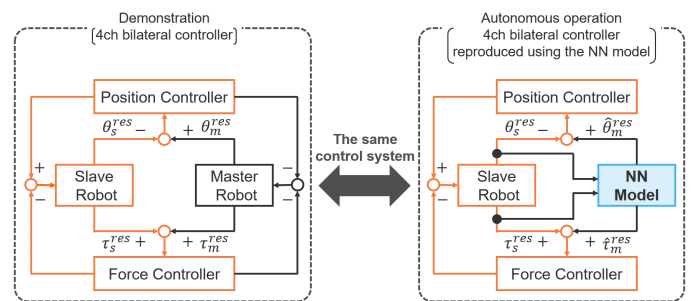


FIGURE 2. Four-channel bilateral controller. The left figure shows a four-channel bilateral controller that was used in the demonstrations. The right figure represents a situation of autonomous operation. In autonomous operations, the master robot and master controllers were substituted by an NN model to mimic the master responses. Note that the systems including the slave robot and slave controllers (orange lines) are the same in both figures.

TABLE 2. Gain of robot controller

K_p	Position feedback gain	121
K_d	Velocity feedback gain	22.0
K_f	Force feedback gain	1.00
g	Cut-off frequency of pseudo derivative [rad/s]	40.0
g_{DOB}	Cut-off frequency of DOB [rad/s]	40.0
g_{RFOB}	Cut-off frequency of RFOB [rad/s]	40.0

B. CONTROLLER

This robot can measure the joint angles of the first to third joints and calculate the angular velocity and torque response using pseudo-differentiation and a reaction force observer (RFOB) [28], respectively. Acceleration control was realized using a disturbance observer (DOB) [29]. A position controller and a force controller were implemented in the robot; these two controllers were composed of a proportional and differential position controller and a proportional force controller, respectively. Herein, θ , $\dot{\theta}$, and τ represent the joint angle, angular velocity, and torque, respectively, and the superscripts cmd , res , and ref indicate the command, response, and reference values, respectively. The torque reference of the slave controller τ_s^{ref} is given as follows:

$$\tau_s^{ref} = J(K_p + K_d s)(\theta_s^{cmd} - \theta_s^{res}) + K_f(\tau_s^{cmd} - \tau_s^{res}), \quad (1)$$

where θ_s and τ_s are the slave variables, defined as follows:

$$\theta_s = \begin{bmatrix} \theta_{s1} \\ \theta_{s2} \\ \theta_{s3} \end{bmatrix}, \quad \tau_s = \begin{bmatrix} \tau_{s1} \\ \tau_{s2} \\ \tau_{s3} \end{bmatrix}. \quad (2)$$

In addition, $J = \text{diag}[J_1, J_2, J_3]$. Here, s is the Laplace operator. In addition, the parameters K_p , K_d , and K_f are the proportional position gain, derivative position gain, and proportional force gain, respectively.

Bilateral control is a remote operation technology between two robots. The operator first operates the master robot and then operates the slave robot directly through the master robot [18] [19]. The operation and reaction forces can be independently measured by the master and slave. This controller was implemented to imitate human object



FIGURE 3. Data collection using four-channel bilateral control

manipulation skills. A four-channel bilateral controller was implemented similar to that in [24].

A block diagram of the four-channel bilateral controller in the demonstration (the data collection phase) is shown on the left side of Fig. 2. The command values of the slave robot in the four-channel bilateral control are given as follows:

$$\theta_s^{cmd} = \theta_m^{res}, \tau_s^{cmd} = -\tau_m^{res}, \quad (3)$$

where θ_m and τ_m are the master variables defined as follows:

$$\theta_m = \begin{bmatrix} \theta_{m1} \\ \theta_{m2} \\ \theta_{m3} \end{bmatrix}, \tau_m = \begin{bmatrix} \tau_{m1} \\ \tau_{m2} \\ \tau_{m3} \end{bmatrix}. \quad (4)$$

III. IMITATION LEARNING FOR VARIABLE-SPEED OPERATION

We propose a method for generating variable-speed motion that can exceed the speed of the original motion using imitation learning.

A. DATA COLLECTION

Fig. 3 shows the data collection phase. The two robots were used for data collection based on four-channel bilateral control, as described in Section II-A. The objective was to generate motion to quickly or slowly erase a line written using a pencil. Therefore, the operator of the master robot erased the lines using seven different frequencies, i.e., 0.61, 0.85, 1.10, 1.22, 1.47, 1.59, and 1.83 Hz. Frequency adjustment was performed using a metronome. This trial was conducted three times at paper heights of 1.6, 3.9, and 6.3 cm from the surface of the desk. A total of 21 trials were conducted. The saved motion data points were acquired over 15 s in each case, and the joint angle, angular velocity, and torque of the master and slave data were stored at 1 kHz. Training data were obtained by augmenting the collected data 20 times by down-sampling at 50 Hz using the technique described in [30].

In addition, Figs. 4 and 5 show some of the training data of θ_{s1}^{res} and τ_{s1}^{res} for a height of 3.9 cm, respectively. From these figures, when the operating speed changed, it can be confirmed that the required motion and force adjustment differed, although the trajectory was similar. When the operation was the fastest, the torque was the greatest because the inertial force was the highest, whereas the torque decreased with a decrease in the operating frequency. However, when the operation was the slowest, the torque was slightly larger

to compensate for the nonlinearity of the frictional force. This is a major problem, making it difficult to achieve motion generation at variable speeds.

B. TRAINING THE NN MODEL PHASE

In this study, we used a network consisting of a recurrent NN (RNN). An RNN, which has a recursive structure, is a network that holds time-series information. This network has contributed significantly to the fields of natural language processing and speech processing [31] [32], and has recently been widely applied to robot motion planning [33]. However, RNNs are hindered by the vanishing gradient problem, making it difficult to learn long-term data. Long short-term memory (LSTM) refers to an NN that can learn long-term inference [34]. This approach has been improved based on the results of numerous studies and was adopted in this study. To extract the feature values from the response variables that do not depend on time-series information, we implemented a convolutional NN (CNN) prior to the LSTM. We expected that the CNN would extract time-independent transformations such as Jacobian matrices.

The network inputs are $\theta_s^{res}, \dot{\theta}_s^{res}, \tau_s^{res}$, and the frequency command of the first joint, and the outputs are $\hat{\theta}_m^{res}, \hat{\dot{\theta}}_m^{res}$, and $\hat{\tau}_m^{res}$ of each joint in the next step. The variables with $\hat{\circ}$ are estimates given by the NN. The frequency command was designed based on the peak frequency values of the first joint angle of the robot, which was calculated using the FFT. Here, the next step indicates a point in time 20 ms later than the slave data. Autonomous operation was realized by considering the network calculation time required to generate motion online. Thus, the data had 315,000 ($15,000[\text{ms}] / 20[\text{ms}] \times 21[\text{trials}]$) $\times 20[\text{augmentation}]$ input-output samples. In addition, the weights were optimized using the mean square error between the normalized master value and the network output.

Fig. 6 shows the network. The responses $\theta_s^{res}, \dot{\theta}_s^{res}$, and τ_s^{res} of each joint of the slave robot are reshaped into other channels. The reshape was designed to predict the effect of the batch normalization (BN) for each unit dimension. In addition, the mini-batch consisted of 100 random sets of 300 time-sequential samples corresponding to 6 s. The frequency command was manually provided using a keyboard and normalized using max-min normalization. Max-min denormalization was set at the output of the network. In this study, the computer used for training and autonomous operation comprised an Intel Core i7-8700K CPU, 32 GB of memory, and an nVIDIA GTX 1080 Ti GPU.

C. AUTONOMOUS OPERATION PHASE

The right part of Fig. 2 shows a block diagram of the slave robot conducting autonomous execution using the trained NN. In the autonomous operation phase, the demonstrator, master robot, and master controllers were substituted by the trained NN. In this case, the command values are not the true response values of the master, but the estimated values

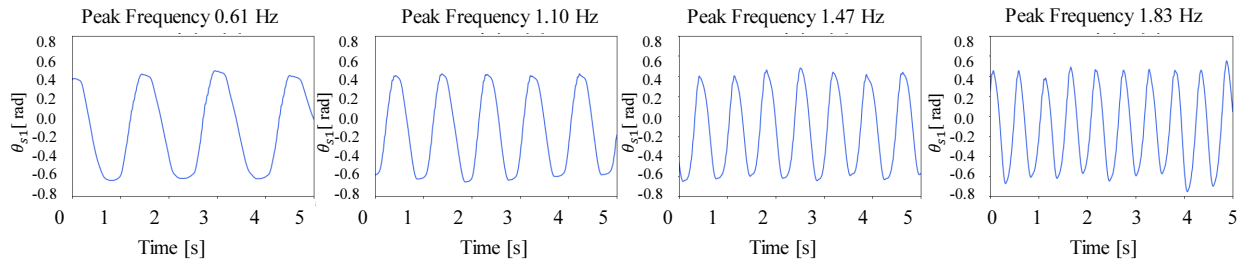


FIGURE 4. θ_{s1}^{res} in training data at each frequency for a height of 3.9 cm. The amplitude of the angular response was almost identical.

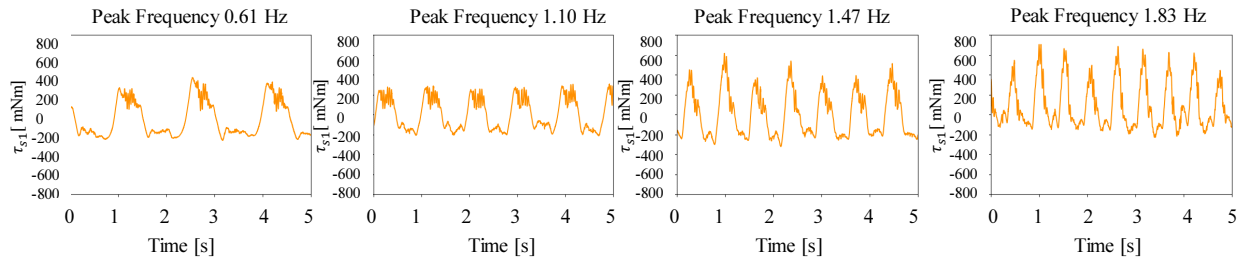


FIGURE 5. τ_{s1}^{res} in training data at each frequency for a height of 3.9 cm. The amplitude of the torque response varied according to the frequency.

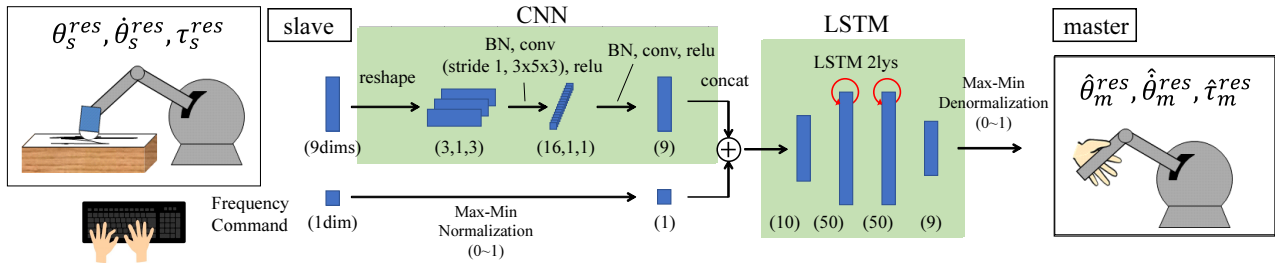


FIGURE 6. Overview of proposed NN using CNN for normalization

provided by the NN.

$$\theta_s^{cmd} = \hat{\theta}_m^{res}, \tau_s^{cmd} = -\hat{\tau}_m^{res} \quad (5)$$

Note that the control system in the autonomous execution phase was the same as that in the data collection phase. Although the input interval into the network was 20 ms, the control period of the position and force controller was 1 ms. Therefore, the control input was updated during every control period.

IV. EXPERIMENT

This section describes the experimental evaluation of the proposed method.

A. PRELIMINARY EXPERIMENT

Prior to performing the main experiment, one of the three conditions described in the introduction was tested. The validity of the predicting command value of the slave, that is, the predicting master response, was evaluated. In this case, the environment was not changed from the data collection phase, the NN was not used, and motion at 2.17 Hz was

simply replayed as a command value. The following two command values for the next step were given for comparison:

- 1) the master's response during the training data (our approach); $\theta_s^{cmd} = \theta_m^{tr}, \tau_s^{cmd} = -\tau_m^{tr}$, and
- 2) the slave's response during the training data; $\theta_s^{cmd} = \theta_s^{tr}, \tau_s^{cmd} = \tau_s^{tr}$.

The variables with superscript *tr* indicate training data. Figs. 7 and 8 show the experimental results for θ_{s1}^{res} and τ_{s1}^{res} , where the blue lines represent the original slave responses in the training data. The orange and gray lines represent the responses reproduced using the master and slave responses in the training data, respectively. The orange lines indicate that the response was almost identical to that of the data collection when the master's next response was used as a command value. However, based on the gray lines, when the next response of the slave was given as a command value, the shape of the response differed significantly from that in the training data. It is evident that the amplitude was smaller than that in the original slave response, and a large phase delay occurred. Given that the motion was rapid, the transfer

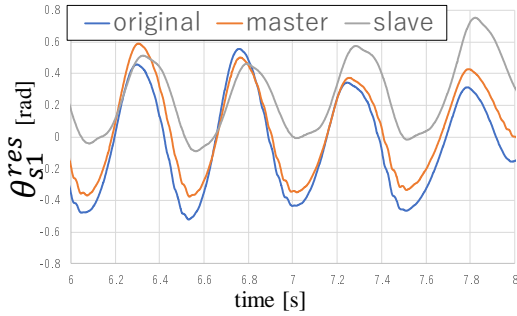


FIGURE 7. Result of θ_{s1}^{res} of preliminary experiment. If and only if we predicted the master values as commands, a fast motion was achieved.

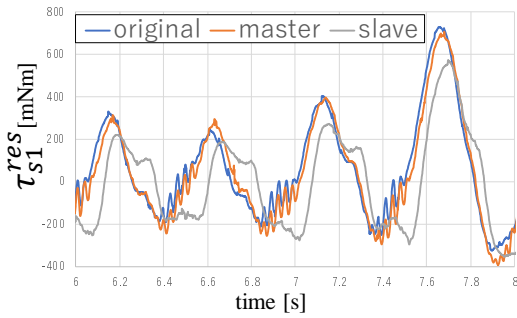


FIGURE 8. Result of τ_{s1}^{res} of preliminary experiment. If and only if we predicted the master values as commands, a fast motion was achieved.

function from the command to the response cannot be 1.

These results clearly show that predicting the master's response is important for reproducing fast motion. Note that the kinesthetic teaching cannot satisfy this condition, nor does conventional imitation learning using bilateral control [20]. As such, temporal reproducibility at high speeds can only be achieved using our approach. Hence, variable speed imitation learning has been made possible for the first time.

B. COMPARATIVE EXPERIMENT

The results from the experiment conducted to change the operating speed based on the training data were compared with the results of a motion copying system [25]. In the latter, the data collected at a frequency of 1.22 Hz and height of 3.9 cm were used to reproduce the operation. Given that the motion copying system simply performs a rescaling of the time axis, it only requires one time series of data for reproduction. To convert the operating speed, the original data were rescaled to fit the target speed data. The training data were rescaled along the time axis of the data using linear interpolation with a zero-order hold.

First, 9 and 16 convoluted channels were compared for the implementation of the CNN. The variable-speed range for 16 channels was wider than that for nine channels. Hence, the proposed method was implemented using 16 channels. The learning required 1500 iterations to obtain a stable training loss for the 16-channel network. The learning time was approximately 40 min.

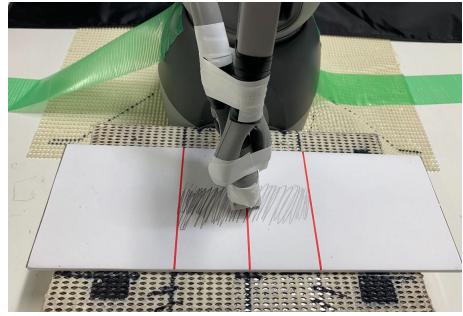


FIGURE 9. Working area. When the robot erased more than 90 % of the area inside the red lines, it was considered a success. Note that we do not intend to erase all of the black lines. However, we investigated whether the robot could erase the arc-shaped area.

C. RESULTS AND DISCUSSION

The success rate of the operation was then evaluated. Fig. 9 shows the working area. Given that this robot was not equipped with a camera, it was not possible to completely erase the entire area. In contrast, it is easy to erase the entire area by combining the proposed method with conventional methods using a camera. However, when several methods are combined, it is difficult to evaluate the effectiveness of the proposed method. Therefore, we investigated whether we could erase the arc-shaped area through which the robot's end-effector passed. When the robot erased more than 90 % of the area inside the red lines, this was defined as successful.

Evaluation was conducted using 15 frequency commands: 0.49, 0.61, 0.73, 0.85, 0.98, 1.10, 1.16, 1.22, 1.34, 1.47, 1.53, 1.59, 1.71, 1.83, and 1.95 Hz, for five heights of 1.6, 2.8, 3.9, 4.9, and 6.3 cm from the surface of the desk. Three trials were conducted for each condition, for a total of 225 trials (15 [frequencies] \times 5 [heights] \times 3 [trials]). Note that height information from the desk surface was not given to the robot. Given that the robot was not equipped with a camera, it needed to adapt to the perturbation of the height using only the angle, angular velocity, and torque information. The experiments can be viewed using the link to a video (<https://youtu.be/GcplxRbnFys>).

Fig. 10 shows the success rate for each height. The blue lines show the success rates of the motion copying system, whereas the orange lines represent the rates of the proposed method. As shown in the figure, the motion copying system performs its task under limited frequencies and heights, whereas the proposed method can adapt to variations in both speed and height. The success rate was the same or higher than that of the motion copying system under all conditions. In particular, given that the motion copying system does not have an adaptation mechanism against a height perturbation, it was significantly less effective at heights of 4.9 and 6.3 cm. Figs. 11- 14 show the angular responses of θ_{s1}^{res} and the torque responses of τ_{s1}^{res} , τ_{s2}^{res} , and τ_{s3}^{res} for a height of 3.9 cm. The blue lines represent the responses of the motion copying system, whereas the orange lines show those of the proposed method. The red lines indicate the working area.

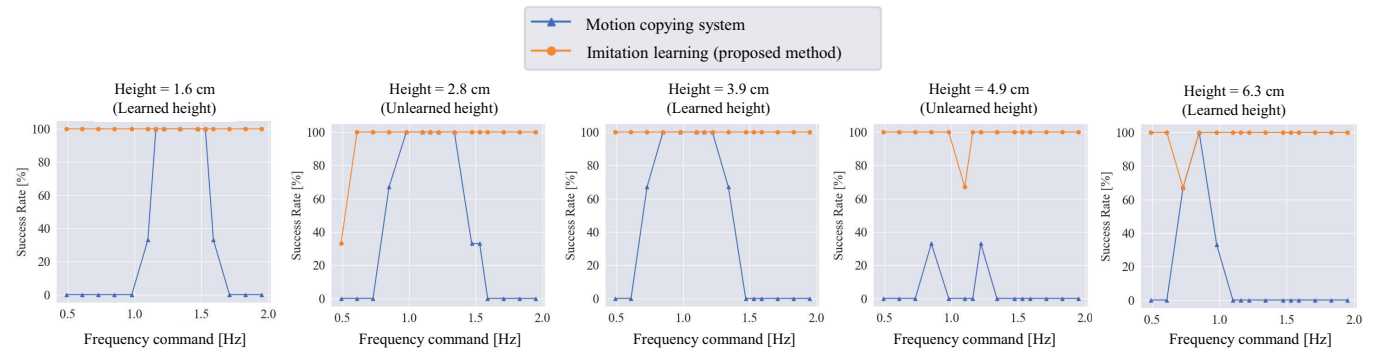
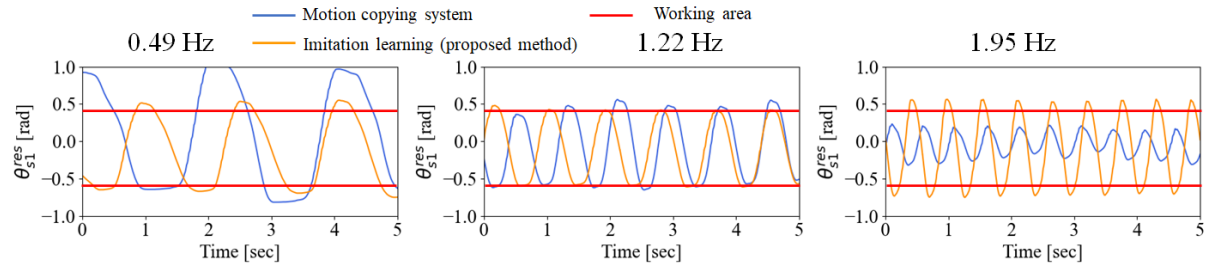
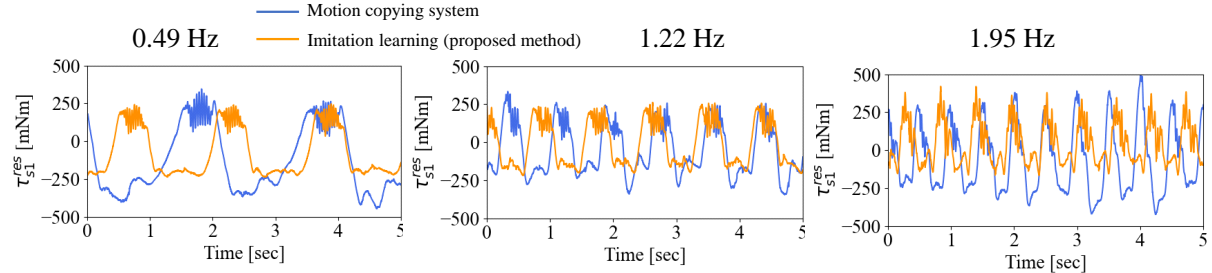


FIGURE 10. Success rate for erasing lines in autonomous operation.

FIGURE 11. Angular response (θ_{s1}^{res}) in autonomous operation, paper height = 3.9 cm (learned height)FIGURE 12. Torque response (τ_{s1}^{res}) in autonomous operation, paper height = 3.9 cm (learned height)

In the motion copying system, within a high-speed range, the amplitude of θ_{s1}^{res} was too small to meet the conditions shown in Fig. 9. In the case of the low-speed range, the amplitude was too large to remain within the desk. On the contrary, the amplitudes of the torque varied adaptively for different frequencies. These figures clearly demonstrate that the proposed method was able to achieve almost the same trajectory regardless of the frequency, whereas the motion copying system exhibited a strong dependency on the frequency. Thus, the proposed method was able to appropriately handle frequency-dependent physical phenomena such as inertial force and friction. The overall success rate of the proposed method was 98.2 %.

Fig. 15 shows the reproducibility of the frequency at a height of 3.9 cm. The horizontal axis shows the frequency command, whereas the vertical axis shows the peak frequency measured using the FFT. Given that the proposed method was 100 % successful, all of the peak frequencies of

θ_{s1}^{res} are plotted. Moreover, four additional experiments were conducted to further evaluate the extrapolation performance of the proposed method. In contrast, given that the conventional method had few successful samples, the behaviors that did not meet the conditions in Fig. 9 are plotted. The blue, orange, and green plots show the peak frequencies of the motion copying system, the proposed method, and the proposed method applied during the additional experiment, respectively. The solid line indicates the identity mapping. When the plots are along the line, this indicates that the reproducibility of the frequency is ideal. In the motion copying system, the operating frequency was adjusted by the designer, and the reproducibility of the operating frequency was consequently high. However, the proposed method was also able to operate at the command frequency, although there were more variations compared to the motion copying system. In the case of extrapolation far from the training data, the reproducibility was reduced, although the peak fre-

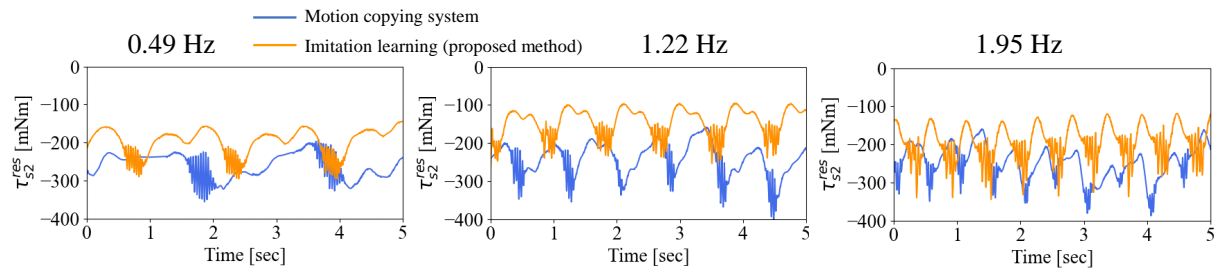


FIGURE 13. Torque response (τ_{s2}^{res}) in autonomous operation, paper height = 3.9 cm (learned height)

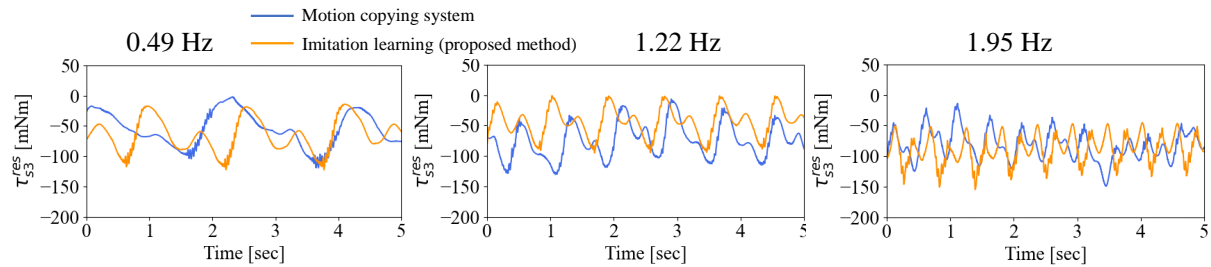


FIGURE 14. Torque response (τ_{s3}^{res}) in autonomous operation, paper height = 3.9 cm (learned height)

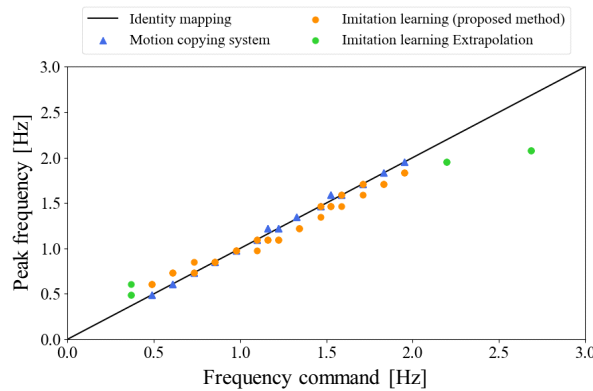


FIGURE 15. Frequency command and actual frequency at a 3.9 cm height in autonomous operation

quency tended to increase with an increase in the frequency command. Note that the operation at 2.08 Hz was achieved using a 2.69 Hz command, indicating that the operation was faster than the fastest training data at 1.83. Thus, the proposed method was not only able to change the operating frequency, but it was also able to perform the task faster than a human. It is also worth noting that the control bandwidth of the robot was approximately 2 Hz, and it would be quite difficult to achieve the desired behavior faster than 2 Hz.

V. CONCLUSION

In this paper, we proposed a method for generating variable-speed motion while adapting to perturbations in the environment. Given that there is a nonlinear relationship between operating speed and frictional or inertial forces, the operating force changes with the work speed. Therefore, we confirmed

that a variable-speed operation could not be achieved using simple interpolation and extrapolation. To solve this problem, we proposed a method to imitate human motion by using four-channel bilateral control, a CNN, and an LSTM. Based on the experimental results, it was determined that the motion was variable to the interpolation of the operating speed of the training data, as well as to the high speed of the extrapolation. Furthermore, the proposed method can complete a given task faster than a human operator. Our future goal is to improve the reproducibility of the frequency during extrapolation.

REFERENCES

- [1] C. Eppner, S. Höfer, R. Jonschkowski, R. Martin-Martin, A. Sieverling, V. Wall, and O. Brock, "Lessons from the amazon picking challenge: Four aspects of building robotic systems," in Proceedings of the Twenty-Sixth International Joint Conference on Artificial Intelligence (IJCAI-17), pp. 4831–4835, 2017.
- [2] E. Brown, N. Rodenberg, J. Amend, A. Mozeika, E. Steltz, M. R. Zakin, H. Lipson, and H. M. Jaeger, "Universal robotic gripper based on the jamming of granular material," Proceedings of the National Academy of Sciences, pp. 18809–018814, 2010.
- [3] S. Levine, P. Pastor, A. Krizhevsky, J. Ibarz, and D. Quillen, "Learning hand-eye coordination for robotic grasping with deep learning and large-scale data collection," The International Journal of Robotics Research, vol. 37, no. 4-5, pp. 421–436, 2017.
- [4] S. Calinon, F. Guenter, and A. Billard, "On learning, representing, and generalizing a task in a humanoid robot," IEEE Transactions on Systems, Man, and Cybernetics, Part B: Cybernetics, vol. 37, no. 2, pp. 286–298, 2007.
- [5] M. Kyarini, M. A. Haseeb, D. Ristic-Durrant, and A. G. P. Graeser, "Robot learning of industrial assembly task via human demonstrations," Autonomous Robots, vol. 43, pp. 239–257, 2019.
- [6] P.-C. Yang, K. Sasaki, K. Suzuki, K. Kase, S. Sugano, and T. Ogata, "Repeatable folding task by humanoid robot worker using deep learning," IEEE Robotics and Automation Letters, vol. 2, no. 2, pp. 397–403, 2016.
- [7] T. Zhang, Z. McCarthy, O. Jow, D. Lee, X. Chen, K. Goldberg, and P. Abbeel, "Deep imitation learning for complex manipulation tasks from virtual reality teleoperation," in Proceedings of 2018 IEEE International Conference on Robotics and Automation (ICRA), pp. 5628–5635, 2018.

- [8] A. Gupta, V. Kumar, C. Lynch, S. Levine, and K. Hausman, "Relay policy learning: Solving long-horizon tasks via imitation and reinforcement learning," arXiv:1910.11956, 2019.
- [9] J. Jiny, L. Petrichy, M. Dehghany, and M. Jagersand, "A geometric perspective on visual imitation learning," in Proceedings of the INternational Conference on Intelligent Robots and Systems, pp. 5194–5200, 2020.
- [10] A. X. Lee, H. Lu, A. Gupta, S. Levine, and P. Abbeel, "Learning force-based manipulation of deformable objects from multiple demonstrations," in 2015 IEEE International Conference on Robotics and Automation, pp. 177–184, 2015.
- [11] P. Kormushev, S. Calinon, and D. G. Caldwell, "Imitation learning of positional and force skills demonstrated via kinesthetic teaching and haptic input," Advanced Robotics, vol. 25, no. 5, pp. 581–603, 2011.
- [12] H. Ochi, W. Wan, Y. Yang, N. Yamanobe, J. Pan, and K. Harada, "Deep learning scooping motion using bilateral teleoperations," in 2018 3rd International Conference on Advanced Robotics and Mechatronics (ICARM), pp. 118–123, 2018.
- [13] L. Rozo, "Interactive trajectory adaptation through force-guided bayesian optimization," in Proceedings of 2019 IEEE/RSJ International Conference on Intelligent Robots and Systems (IROS), p. 7603, 2019.
- [14] T. Osa, N. Sugita, and M. Mitsuishi, "Online trajectory planning and force control for automation of surgical tasks," IEEE Transactions on Automation Science and Engineering, vol. 15, no. 2, pp. 675–691, 2018.
- [15] T. Tsuji, J. Ohkuma, and S. Sakaino, "Dynamic Object Manipulation Considering Contact Condition of Robot with Tool," IEEE Transactions on Industrial Electronics, vol. 63, no. 3, pp. 1972–1980, 2016.
- [16] T. Adachi, K. Fujimoto, S. Sakaino, and T. Tsuji, "Imitation learning for object manipulation based on position/force information using bilateral control," in Proceedings of the 2018 IEEE/RSJ International Conference on Intelligent Robots and Systems, pp. 3648–3653, 2018.
- [17] K. Fujimoto, S. Sakaino, and T. Tsuji, "Time series motion generation considering long short-term motion," in Proceedings of 2019 IEEE/RSJ International Conference on Intelligent Robots and Systems (IROS), pp. 6842–6848, 2019.
- [18] S. Sakaino, T. Sato, and K. Ohnishi, "Multi-dof micro macro bilateral controller using oblique coordinate control," IEEE Transacions on Industrial Informatics, vol. 7, pp. 446–454, July 2011.
- [19] S. Sakaino, T. Furuya, and T. Tsuji, "Bilateral control between electric and hydraulic actuators using linearization of hydraulic actuators," IEEE Transactions on Industrial Electronics, 2017.
- [20] L. Rozo, P. Jimenez, and C. Torras, "A robot learning from demonstration framework to perform force-based manipulation tasks," Intel Serv Robotics, vol. 6, pp. 33–51, 2013.
- [21] S. Sakaino, T. Sato, and K. Ohnishi, "A novel motion equation for general task description and analysis of mobile-haptic," IEEE Transactions on Industrial Electronics, vol. 60, no. 7, pp. 2673–2680, 2013.
- [22] L. Rozo, D. Bruno, S. Calinon, and D. G. Caldwell, "Learning optimal controllers in human-robot cooperative transportation tasks with position and force constraints," in Proceedings of IEEE/RSJ International Conference on Intelligent Robots and Systems, pp. 1024–1030, 2015.
- [23] A. Sasagawa, K. Fujimoto, S. Sakaino, and T. Tsuji, "Imitation learning based on bilateral control for human-robot cooperation," IEEE Robotics and Automation Letters, vol. 5, no. 4, pp. 6169–6176, 2020.
- [24] A. Sasagawa, S. Sakaino, and T. Tsuji, "Motion generation using bilateral control-based imitation learning with autoregressive learning," IEEE Access, vol. 9, pp. 20508–20520, 2021.
- [25] Y. Yokokura, S. Katsura, and K. Ohishi, "Motion copying system based on real-world haptics in variable speed," in Proceedings of 2008 13th International Power Electronics and Motion Control Conference, pp. 1604–1609, 2008.
- [26] J. Tani and M. Ito, "Self-organization of behavioral primitives as multiple attractor dynamics: A robot experiment," IEEE Transactions on Systems, Man, and Cybernetics - Part A: Systems and Humans, vol. 33, no. 4, pp. 481–488, 2003.
- [27] T. Yamazaki, S. Sakaino, and T. Tsuji, "Estimation and kinetic modeling of human arm using wearable robot arm," Electrical Enginnering in Japan, vol. 199, no. 3, pp. 57–67, 2017.
- [28] T. Murakami, F. Yu, and K. Ohnishi, "Torque sensorless control in multidegree-of-freedom manipulator," IEEE Transactions on Industrial Electronics, vol. 40, no. 2, pp. 259–265, 1993.
- [29] K. Ohnishi, M. Shibata, and T. Murakami, "Motion control for advanced mechatronics," IEEE/ASME Transactions on Mechatronics, vol. 1, no. 1, pp. 56–67, 1996.
- [30] R. Rahmatizadeh, P. Abolghasemi, A. Behal, and L. Böloni, "From virtual demonstration to real-world manipulation using lstm and mdn," arXiv:1603.03833, 2016.
- [31] M. Sundermeyer, H. Ney, and R. Schluter, "From feedforward to recurrent lstm neural networks for language modeling," IEEE/ACM Transactions on Audio, Speech, and Language Processing, vol. 23, no. 3, pp. 517–529, 2015.
- [32] Y. Zhang, G. Chen, D. Yu, K. Yaco, S. Khudanpur, and J. Glass, "Highway long short-term memory rnns for distant speech recognition," in Proceedings of 2016 IEEE International Conference on Acoustics, Speech and Signal Processing, pp. 5755–5759, 2016.
- [33] Z. Zhang, L. Zheng, J. Yu, Y. Li, and Z. Yu, "Three recurrent neural networks and three numerical methods for solving a repetitive motion planning scheme of redundant robot manipulators," IEEE/ASME Transactions on Mechatronics, vol. 22, no. 3, pp. 1423–1434, 2017.
- [34] S. Hochreiter and J. Schmidhuber, "Long short-term memory," Neural Computation, vol. 9, no. 8, pp. 1735–1780, 1997.



SHO SAKAINO Sho Sakaino obtained the B.E. degree in system design engineering and the M.E. and Ph.D. degrees in integrated design engineering from Keio University, Yokohama, Japan, in 2006, 2008, and 2011 respectively. He was an assistant professor at Saitama University from 2011 to 2019. Since 2019, he has been an associate professor at University of Tsukuba. His research interests include mechatronics, motion control, robotics, and haptics. He received the IEEE Industry Application Society Distinguished Transaction Paper Award in 2011 and 2020. He also received the RSJ Advanced Robotics Excellent Paper Award in 2020.



KAZUKI FUJIMOTO received the B.E. and M.E. degrees in electrical and electronic system engineering from Saitama University, Saitama, Japan, in 2018 and 2020, respectively.



YUKI SAIGUSA received the B.E. degree in electrical and electronic system engineering from Saitama University, Saitama, Japan, in 2020. He is currently working toward M.E. degrees in the Graduate School of Science and Technology, degree programs in intelligent and mechanical interaction systems, University of Tsukuba, Japan.



TOSHIAKI TSUJI received the B.E. degree in system design engineering and the M.E. and Ph.D. degrees in integrated design engineering from Keio University, Yokohama, Japan, in 2001, 2003, and 2006, respectively. He was a Research Associate in the Department of Mechanical Engineering, Tokyo University of Science, from 2006 to 2007. He is currently an Associate Professor in the Department of Electrical and Electronic Systems, Saitama University, Saitama, Japan. His research interests include motion control, haptics, and rehabilitation robots. Dr. Tsuji received the FANUC FA and Robot Foundation Original Paper Award in 2007 and 2008. He also received the RSJ Advanced Robotics Excellent Paper Award and the IEEJ Industry Application Society Distinguished Transaction Paper Award in 2020.

• • •